Iranian Journal of Analytical Chemistry

Journal home page: http://ijac.journals.pnu.ac.ir

Fast Removal of Reactive Red 141 and Reactive Yellow 81 From Aqueous Solution by Fe_3O_4 Magnetic Nanoparticles Modified With Ionic Liquid 1-Octyl-3-methylimidazolium Bromide

Sedigheh Kamran*, Hossein Tavallali, Ali Azad

Department of Chemistry, Payame Noor University, P. O. Box 19395-3697 Tehran, Iran.
*E-mail: kamran_ss5@yahoo.com & s.kamran@pnu.ac.ir

Received 12 June 2014; Received in revised form 25 August 2014; Accepted 2 September 2014, Online published: 1 October 2014

ABSTRACT

Fe_3O_4 magnetic nanoparticles modified with 1-Octyl-3-methylimidazolium bromide ([C_8MIM]-Fe_3O_4) were used for the removal of reactive red 141 (RR141) and reactive yellow 81 (RY81) as model azo dyes from aqueous solution. The mean size and the surface morphology of the nanoparticles were characterized by TEM, XRD and FTIR techniques. Adsorption studies of two dyes were performed under different experimental conditions in batch technique. The adsorption of dyes onto [C_8MIM]-Fe_3O_4 nanoparticles was affected by the initial pH, dye concentration, adsorbent amount, contact time and temperature. Experimental results indicated that [C_8MIM]-Fe_3O_4 nanoparticles removed more than 98%. The maximum adsorption capacity of [C_8MIM]-Fe_3O_4 for the Langmuir model was 71.4 mg g^{-1} and 62.5 mg g^{-1} for RR141 and RY81, respectively. The isotherm evaluations revealed that the Langmuir model attained better fits to the equilibrium data than the Freundlich model. Adsorption processes onto [C_8MIM]-Fe_3O_4 nanoparticles were spontaneous exothermic and endothermic for RY81 and RR141, respectively. Dyes were desorbed from nanoparticles by NaCl solution 0.1 mol L^{-1} at 80 and 30 °C for RR141 and RY81, respectively.

KEYWORDS: Magnetic Nanoparticle; Ionic Liquid; Adsorption; Azo Dye.

1. INTRODUCTION

Various kind of synthetic dyes are found in the effluents of waste water in the dyestuff textile, leather paper and plastic industries. Dyes removed from wastes, has been the target of great attention in the past few years, not only because of potential toxicity of dyes, but mainly due to visibility problems. Unfortunately, azo dyes with aromatic structures are comprised of recalcitrant molecules and are resistant to aerobic digestion and are stable in oxidizing agent. In general, the reactive dyes are the most problematic among other dyes as they remain unaffected through conventional treatment systems. The decolourization of dye effluents has received increasing attention, thus various chemical, physical and biological treatment methods have been developed for the removal of dyes from aqueous solution, including precipitation, coagulation, flocculation, reverse osmosis, degradation, anion exchanging, membrane separation and bacterial cells application [1-3]. Adsorption has proven to be a reliable treatment methodology due to its low capital investment cost, simplicity of design, ease of operation and insensitivity to toxic substances, but its application is limited by the high price of some adsorbent and the large amount of waste water normally involved. Activated carbon [4-5], mesoporous carbon [6], clay minerals [7], hydrotalcite [8], biopolymers such as chitosan beads [9] and agricultural by products [10-11] are among the adsorptive materials that have been tested for the treatment of waste waters. In this regard, much attention has recently been paid to nanotechnology [12]. Nanomaterials have large specific surface areas and thus a large fraction of active sites are available for appropriate chemical interaction. The use of synthetic iron oxides is much more economical than commercial efficient activated carbon in the relative ratio depending on the particular kind of activated carbon [13].

This paper focuses on the preparation of magnetic nanoparticles of Fe_3O_4 modified by 1-Octyl-3-methylimidazolium bromide (C_8MIM-Fe_3O_4) and characterization by Transmission electron microscopy (TEM), X-ray diffraction (XRD), Fourier transform infrared (FTIR) spectroscopy. Removal of reactive red 141 (RR141) and reactive yellow 81 (RY81) Table 1, were studied as model azo dyes with different functional groups. The effects of different experimental conditions such as amount of [C_8MIM]-Fe_3O_4 nanoparticles, concentrations of dyes, pH of the aqueous

Table 1. Some characteristics of the investigated dyes.

Characteristic	RR 141	RY 81
Molecular formula	$C_{52}H_{26}Cl_2N_{14}Na_8O_{26}S_8$	$C_{52}H_{34}Cl_2N_{18}Na_6O_{20}S_6$
Color index name	Reactive Red 141	Reactive Yellow 81
Molecular weight	1774.19 (g mol^{-1})	1632.18 (g mol^{-1})
λ_{max}	548 (nm)	401 (nm)
Class	Diazo (-N=N- bond)	Diazo (-N=N- bond)
Chemical structure	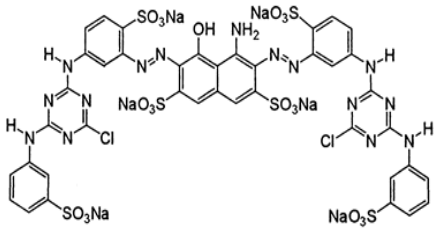	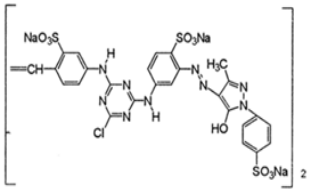

sample and contact times, on removal of both dyes were evaluated. Adsorption isotherms and thermodynamic parameters were characterized as well**.**

2. EXPERIMENTAL

2.1. Chemicals and reagents

Analytical grades of reactive red 141, reactive yellow 81, sodium hydroxide solution (1.5 mol L^{-1}), hydrochloric acid (37 %w/w), acetone, acetic acid (99.9 %w/w), $FeCl_3.6H_2O$ (96 %w/w) and $FeSO_4 \cdot 7H_2O$ (99.9 %w/w) were purchased from Merck. Stock solutions (1000 mg L^{-1}) of RR141 and RY81 were prepared. For treatment experiments, the dye solutions with concentrations in the range of 40-120 mg L^{-1} were prepared by successive dilution of the stock solution with distilled water. The pH adjustments were performed with HCl and NaOH solutions (0.01-1.0 mol L^{-1}). Ionic liquid 1-octyl-3-methylimidazolium bromide, [C_8MIM][Br], was prepared according to the procedure reported in the literature [14].

2.2. Apparatus

A double beam UV-visible Shimadzu spectrophotometer equipped with a 1-cm quartz cell was used for recording the visible spectra and absorbance measurements. The XRD measurements were performed on an XRD Bruker D8 Advance. The FTIR spectra were recorded on a Shimadzu FTIR 8000 spectrometer. A transmission electron microscope (Philips CM 10 TEM) was used for recording the TEM images. A Metrohm 692 pH meter was used for monitoring the pH values. A water Ultrasonicator (sonic vcx750, USA) was used to disperse the nanoparticles in solution and a super magnet Nd–Fe–B (1.4 T, 10×5×2 cm) was used. All measurements were performed at ambient temperature.

2.3 Preparation of ionic liquid-modified magnetic nanoparticles

The nanoparticles of Fe_3O_4 were synthesized by mixing ferrous sulfate and ferric chloride in NaOH solution with constant stirring as recommended [15]. To obtain maximum yield for magnetic nanoparticles during co-precipitation process, the molar ratio of Fe^{2+}/Fe^{3+} was about 0.5. The precipitate was heated at 80°C for 30 minutes and was sonicated for 20 minutes, then washed three times with 50 mL distilled water.

Modification of Fe_3O_4 nanoparticles was carried out using ionic liquid [C_8MIM][Br] under vigorous magnetic stirring for 30 minutes at 50°C. The modified iron oxide nanoparticles ([C_8MIM]-Fe_3O_4) were collected by applying a magnetic field with an intensity of 1.4 T. The [C_8MIM]-Fe_3O_4 nanoparticles were washed three times with distilled water with a total volume of 150 mL. Nanoparticles and distilled water mixture was dispersed by ultrasonicator for 10 minutes at room temperature. Then, the [C_8MIM]-Fe_3O_4 nanoparticles were magnetically separated.

2.4. Characterization of Fe_3O_4 and [C_8MIM]-Fe_3O_4

The peaks positions and relative intensities observed in XRD patterns of [C_8MIM]-Fe_3O_4 nanoparticles and standard Fe_3O_4 are shown in Fig. 1 for comparison.

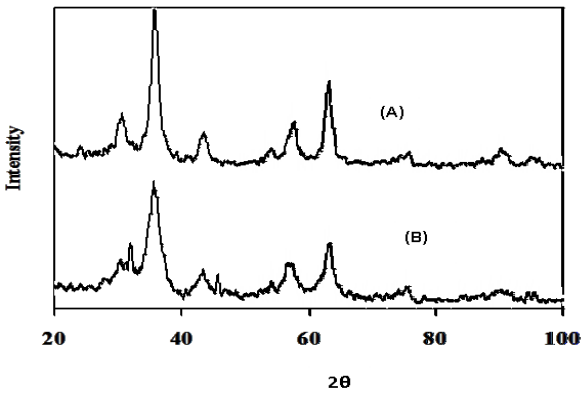

Fig. 1. XRD pattern of Fe_3O_4, A; and [C_8MIM]-Fe_3O_4, B.

Although the magnetic nanoparticles surfaces in [C_8MIM]-Fe_3O_4 were coated with ionic liquid, analysis of XRD patterns of Fe_3O_4 and [C_8MIM]-Fe_3O_4 indicated very distinguishable peaks for magnetite crystal, which means that these particles have phase stability [16-17].

The FTIR spectra of Fe_3O_4, ionic liquid and [C_8MIM]-Fe_3O_4 are shown in Fig. 2A-2C. In the case of Fe_3O_4, the broad absorption band at 3440 cm^{-1} indicates the presence of surface hydroxyl groups (O–H stretching) and the bands at low wave numbers ($\leq$ 700 cm^{-1}) are related to vibrations of the Fe-O bonds in iron oxide.

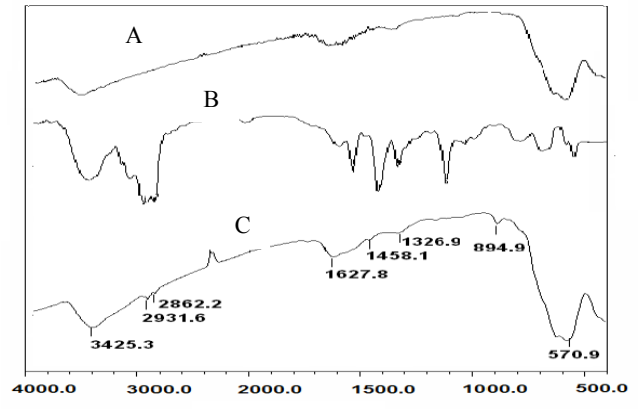

Fig. 2. FTIR spectra of Fe_3O_4, A; IL, B; and [C_8MIM]-Fe_3O_4, C.

The presence of magnetite nanoparticles can be verified by appearance of two strong absorption bands around 632 and 585 cm^{-1} [18-19]. The Fe-O bond peak of the bulk magnetite is observed at 570.9 cm^{-1}. In the spectrum of ionic liquids (Fig. 2A-2C), a long hydrocarbon chain in [C_8MIM][Br] gives significantly stronger peaks in the ranges of 2800-3100 and 1465-1640 cm^{-1}. In the FTIR spectrum of [C_8MIM]-Fe_3O_4, the significant absorption band at 2931.6 cm^{-1} is due to the C-H stretching. The absorption band indicates to the C-N stretching in [C_8MIM]-Fe_3O_4 at 1458.1 cm^{-1}.

Fig. 3A is the representative TEM image of Fe_3O_4 nanoparticles. The average diameter of Fe_3O_4 nanoparticles was about ~10 nm. However, the TEM image (Fig. 3B) indicates that [C_8MIM]-Fe_3O_4 (13-15 nm) had a larger particle diameter than Fe_3O_4. If it is assumed that the difference of 3-5 nm in the mean sizes of both nanoparticles is significant, it revealed that ionic liquid caused agglomeration of Fe_3O_4 nanoparticles. The ionic liquids could reduce the surface charges of nanoparticles; a case similar to what can be observed for colloidal particles when an inert electrolyte is added to their aqueous solutions. The experimental curves corresponding to the immersion technique [20-21] were obtained for four sorbents and are presented in Fig. 4 Suspensions of 5.5 g L^{-1} of individual sorbents were prepared and were put into contact with 0.10 mol L^{-1} NaCl solutions adjusted at different pH values. The aqueous suspensions were agitated for 48 hours until the equilibrium pH was achieved.

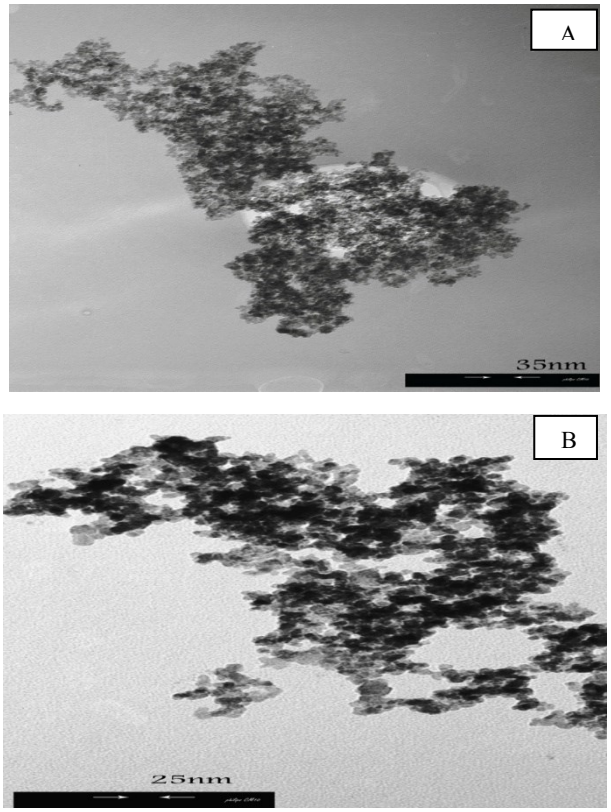

Fig. 3. The TEM image of Fe_3O_4, A; and [C_8MIM]-Fe_3O_4, B.

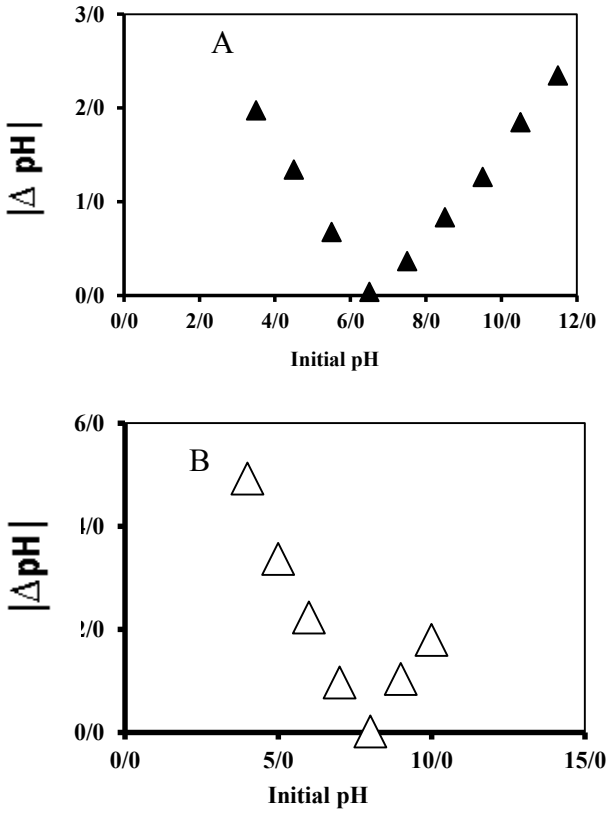

Fig. 4. Immersion technique curves of Fe_3O_4, A; and [C_8MIM]-Fe_3O_4, B.

The pH value at the point of zero charge (pH_{pzc}) was determined by plotting the difference of final and initial pHs (ΔpH) versus the initial pH. As it is shown in Fig. 4, the pH_{pzc} value for Fe_3O_4 and $[C_8MIM]$-Fe_3O_4 nanoparticles are 6.5 and 8.0, respectively, which means that the pH of Fe_3O_4 has shifted from 6.5 to 8.0 after modification with ionic liquid. This confirmed the deposition of ionic liquid onto the surface of Fe_3O_4 and also revealed that $[C_8MIM]$-Fe_3O_4 was positively charged at pH < 8.0.

2.5. Dye removal experiments

Dye-removal ability of the synthesized $[C_8MIM]$-Fe_3O_4 was carried out by using batch technique for individual dye based on a procedure described as follows. Aliquots of 15 mL of the individual dye solutions with initial concentrations of 40-120 mg L^{-1} in the pH range of 3.0-12.0, adjusted by 0.l0 mole L^{-1} of HCl and NaOH solutions were prepared and transferred into individual beaker. A known amount of $[C_8MIM]$-Fe_3O_4 in the range of 5-25 mg was added to each solution and the suspension was immediately stirred with a magnetic stirrer for a predefined time of 5 minutes (equilibrium time). The solid phases, containing adsorbed dye on the surface of $[C_8MIM]$-Fe_3O_4 nanoparticles, were magnetically separated. The aqueous phases were analyzed for finding the residual dye concentration by measuring absorbance at 548 and 401 nm for RR141 and RY 81, respectively. The percent adsorption of dye, i.e. the dye-removal efficiency of $[C_8MIM]$-Fe_3O_4, was determined by using the following equation:

$$\text{Dye removal efficiency (\%)} = \frac{C_0 - C_f}{C_0} \times 100$$

where C_0 and C_f represent the dye concentrations (in mg L^{-1}) before and after adsorption, respectively. All tests were performed in duplicate at ambient temperature. The amount of suspension of $[C_8MIM]$-Fe_3O_4 nanoparticles after dye adsorption was magnetically separated and mother solution was spectrophotometrically analyzed for ionic liquid. The results revealed that no leaching of ionic liquid had occurred from the surface of nanoparticles.

3. RESULTS AND DISCUSSION

The efficiency of the prepared $[C_8MIM]$-Fe_3O_4 as adsorbents for removal of RR141 and RY81 from their individual aqueous solutions was investigated under different experimental condition in order to find their optimum values as discussed below.

3.1. Effect of solution pH

Solution pH is an important parameter that affects adsorption of dye molecules [22]. The effect of the initial pH of the solution on the adsorption of RR141 (50 mg L^{-1}) and RY81 (70 mg L^{-1}), from their individual solutions, onto $[C_8MIM]$-Fe_3O_4 nanoparticles (with a dosage of 10 mg) was assessed at different pH conditions, ranging from 2.0 to 11.0 by using batch technique. Each solution was stirred for a period of 5 minutes and the results are shown in Fig. 5.

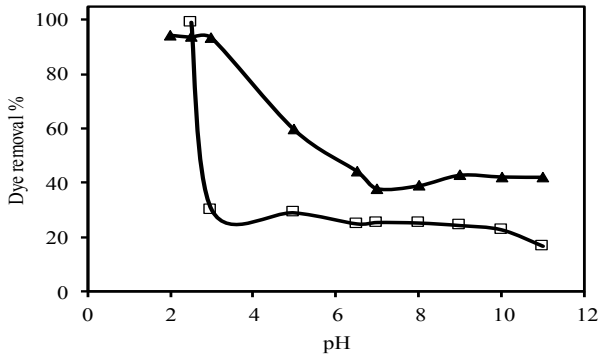

Fig. 5. Effect of initial pH of dye solution on removal of RR 141 (▲) and RY 81(□). Experimental conditions: $[C_8MIM]$-Fe_3O_4 amount of 10 mg, initial concentration of RR141 (50 mg L^{-1}) and RY81 (70 mg L^{-1}), stirring time of 5 minutes.

Fig. 5 shows that the initial pH of the sample solution could significantly affect the extent of adsorption of both dyes. Since the populations of negatively-charged nanoparticles are expected to be increased by increasing pH, the percent removal of dyes is firstly increased as long as the dyes molecules are present in their positive or neutral forms which are the case in the pH values lower than ~ 2.0. At pH more than 2.5, the anionic form of both dyes predominates and electrostatic repulsions are developed between both negatively-charged nanoparticles and dyes molecules. The results of this experiment, Fig. 5, indicate that there is a decrease in percent removal of each dye as pH increases to the values more than 2.5. A color change was observed at high pHs that could be due to the decomposition of the dye.

Generally, the higher adsorption of dyes at lower pH conditions could be due to the electrostatic attractions between negatively-charged dyes anions and the positively-charged nanoparticles, whereas at higher pH conditions the abundance of OH^- are expected to prevent the adsorption of the anionic forms of the dyes [23]. Similar results have been reported for the adsorption of other reactive dyes from aqueous solutions [24].

It should be mentioned that the value of pH_{pzc} (6.5), as reported [25], revealed that the deposition of ionic liquid onto the surface of Fe_3O_4 produces $[C_8MIM]$-Fe_3O_4 with more positive charges at pH < 8.

3.2. Effect of $[C_8MIM]$-Fe_3O_4 dosage

The effect of $[C_8MIM]$-Fe_3O_4 dosage on adsorption of RR141 and RY81, from their individual solutions, was investigated using a batch technique by adding a known quantity of the adsorbent, in the range of 5-25 mg, into individual beakers containing 10 mL of the dye solution. The resulted suspensions were immediately stirred with a magnetic stirrer for 5 minutes. After the mixing time elapsed, the $[C_8MIM]Fe_3O_4$ nanoparticles were magnetically

separated and the solutions were analyzed for the dye residue. For all measurements, the initial dyes concentrations were fixed at 50 mg L^{-1} for RR141 and at 70 mg L^{-1} for RY81 while the value of pH was 2.5. Results in Fig. 6 indicate that 96% of RR141 and 95% of RY81 were removed from their individual aqueous solutions when an initial amount of 10 mg [C_8MIM]-Fe_3O_4 was used. The percent removals of both dyes increased with increasing [C_8MIM]-Fe_3O_4 (up to the amount of 10 mg) and eventually reached to the values of 99.7% and 98.8% for RY 81 and RR14, respectively. Further increase in the adsorbent dosage did not affect the removal of dyes. Hence, the optimum amount of [C_8MIM]-Fe_3O_4 nanoparticles for removing 50 mg L^{-1} RR 141 and 70 mg L^{-1} RY81 from their individual aqueous solutions was found to be 10 mg. This observation can be explained by the fact that more adsorption sites would be available for dye molecules at higher amount of [C_8MIM]-Fe_3O_4. However, any decreases in adsorption, with increasing the amount of Fe_3O_4, could be attributed to the aggregation of adsorption sites, leading to a decrease in surface area of nanoparticles [26].

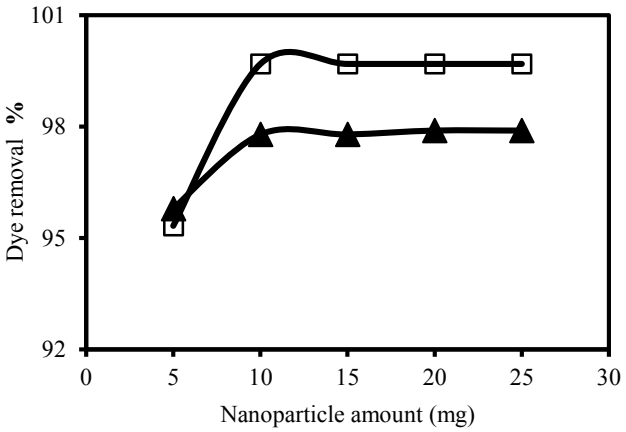

Fig.6. Effect of initial amount of [C_8MIM]-Fe_3O_4 nanoparticles on removal of RR141 (▲) and RY 81 (□). Experimental conditions: pH 2.5, initial concentration of RR 141(50 mg L^{-1}) and RY81 (70 mg L^{-1}), stirring time of 5 minutes.

3.3. Effect of solution temperature

The effect of temperature on the adsorption of RR 141 (50 mg L^{-1}) and RY81 (70 mg L^{-1}) from their individual solutions on 10 mg of [C_8MIM]-Fe_3O_4 nanoparticles was studied at pH 2.5 with a stirring time of 5 minutes. A thermo shaker was used for adjusting of temperature and shaking. Fig. 7 shows the removal efficiencies for both dyes as a function of temperature ranging between 293 and 343 K.

The results indicate that solution temperature strongly affected the adsorption efficiency of RY81. For instance, the adsorption efficiency of RY 81 was 99% at 293 K, but it decreases to 79% at 343 K indicating to an exothermic nature of the adsorption process. However, in comparison with RY81, adsorption efficiency of RR141 was 91% at 293 K; it increases to 98% at 343 K which indicates to the presence of an endothermic nature for the RY adsorption.

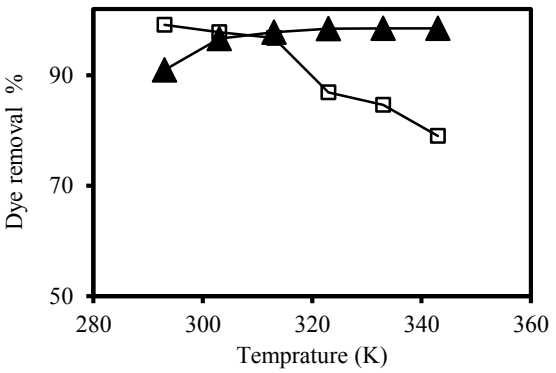

Fig. 7. Effect of temperature on removal of RR141 (▲) and RY 81 (□). Experimental conditions: pH 2.5, initial concentration of RR 141 (50 mg L^{-1}) and RY81 (70 mg L^{-1}), stirring time of 5 minutes.

The changes in standard free energy as well as changes in enthalpy and entropy of adsorption were calculated using van't Hoff equation:

$$\Delta G^0 = -RT \ln K_c$$

$$\ln K_c = -\frac{\Delta H^0}{RT} + \frac{\Delta S^0}{R}$$

Where ΔS° and ΔH° are change in entropy and enthalpy of adsorption, respectively. The K_c is the ratio of adsorbate concentration on adsorbent at equilibrium (q_e) to the remaining adsorbate concentration in the solution at equilibrium (C_e). The values of ΔH° and ΔS° were evaluated from the slope and intercept of van't Hoff plot (Table 2). The results indicate that the adsorption processes for RR141 and RY81 are endothermic and exothermic, respectively. The negative value of ΔG° indicates that the adsorption processes for both dyes are spontaneous. The direct dependency of the negative value of ΔG° to temperature indicates that the spontaneity of adsorption is proportional to temperature. The value of ΔG° obtained in this study indicates that the physisorption is the dominating mechanism; it is well-known that the absolute value of change in free energy for a physisorption process is between 20 and 0 kJ mol^{-1} while it is in the range of 80 to 400 kJ mol^{-1} for a chemisorptions process [27-28]. The values of entropy for adsorption of RR141 and RY81 were 118.8 and −185.2 J mol^{-1} K^{-1}, respectively. The positive value of ΔS° suggests randomness increasing at the solid/solution interface during the adsorption of RR141. Inversely, the negative value of ΔS° indicates a decrease in randomness at the solid/solution interface during the adsorption of RY81 onto [C_8MIM]-Fe_3O_4 nanoparticles [22,29,30].

3.4. Effect of contact time

The contact time (stirring time) between adsorbate and adsorbent is one of the most important parameter that affects the performance of adsorption processes.

Table 2. Thermodynamic parameters of dyes-adsorption process onto [C8MIM]-Fe_3O_4 nanoparticles.

Dye	ΔS_0^T (J mol^{-1} K^{-1})	ΔH_0^T(kJ mol^{-1})	ΔG_0^T(kJ mol^{-1})					
			293K	303K	313K	323K	333K	343K
RR141	118.8	30.4	-4.4	-5.5	-6.7	-7.9	-9.1	-10.3
RY81	-185.2	-64.3	-10.0	-8.2	-6.3	-4.4	-2.6	-1.2

The effect of contact time on the performance of [C_8MIM]-Fe_3O_4 nanoparticles for adsorption of both dyes was investigated. A [C_8MIM]-Fe_3O_4 amount of 10 mg and a solution pH of 2.5 were considered for following this investigation. The initial dyes concentrations for all tested solutions were 40 and 70 mg L^{-1} for RR141 and RY81, respectively. Fig. 8 shows removal efficiencies for both dyes as a function of stirring time in the range of 5-25 minutes. The results indicate that the adsorption processes for both dyes started immediately upon addition of [C_8MIM]-Fe_3O_4. The removal efficiency for RY rapidly increased from 98%, in the first minute of contact, to a value of 99% after stirring time of 2 minutes where the equilibrium condition was attained. For RR141, the percentage of removal, obtained in the first minute of stirring, was 95%; complete removal was attained when the stirring was done for 4 minutes. Therefore, the optimum contact time between sample solution and [C_8MIM]-Fe_3O_4 nanoparticles was considered to be 2 and 4 minutes for RY81 and RR141, respectively. The rapid adsorption, at the initial contact time, is due to the availability of fresh positively-charged surfaces of adsorbent which led to a fast electrostatic adsorption of the ionic dyes molecules from the solution [13]. The presence of ionic liquid onto the surface of nanoparticles increases both electrostatic and hydrophobic interactions between [C_8MIM]-Fe_3O_4 and dyes which consequently increases both rate of dye-adsorption process and dye-removal efficiency. This also shortens the contact time required for dyes to be quantitatively removed by [C_8MIM]-Fe_3O_4 [31].

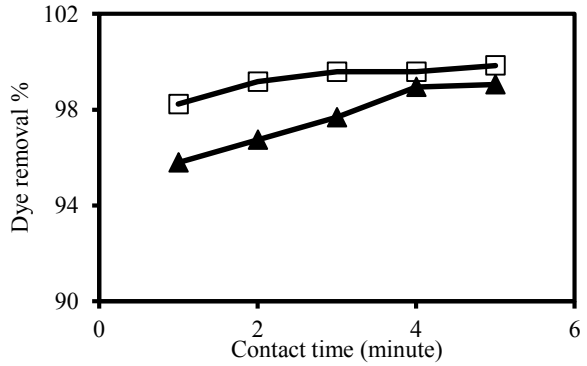

Fig. 8. Effect of stirring time on removal of RR141 (▲) and RY 81(□). Experimental conditions: [C_8MIM]-Fe_3O_4 amount of 10 mg, pH 2.5, initial concentration of RR 14,150 mg L^{-1}) and RY81 (70 mg L^{-1}).

3.5. Effect of dye concentration

The initial dye concentration is an important parameter that can affect its adsorption process. This will determine the concentration range of dye that could be quantitatively adsorbed, i.e. the concentration range for which the adsorption efficiency is high and independent of the initial concentration of dye. To obtain this, different concentrations of RR141 and RY81 dyes were studied for their removal by [C_8MIM]-Fe_3O_4 under optimum experimental conditions. The results, in terms of removal efficiency versus initial concentrations of dyes, are shown in Fig. 9. The results indicate that [C_8MIM]-Fe_3O_4 nanoparticles have greater capacity for adsorption of RR141 than RY81.

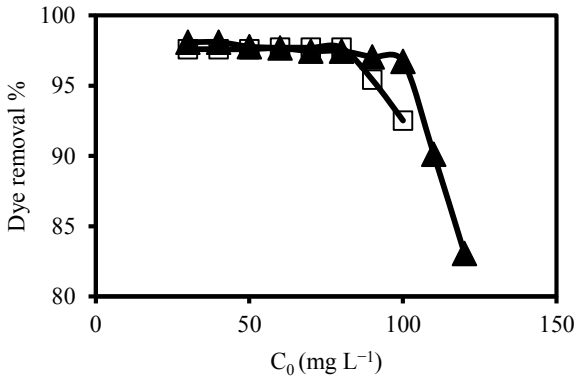

Fig. 9. Effect of initial dye concentration on removal of RR141 (▲) and RY 81 (□). Experimental conditions: [C_8MIM]-Fe_3O_4 amount of 10 mg, pH 2.5, initial concentration of RR 141(50 mg L^{-1}) and RY81 (70 mg L^{-1}), stirring time of 5 minutes.

3.6. Adsorption isotherm modeling

The equilibrium relationship between the quantity of adsorbate per unit of adsorbent (q_e) and its equilibrium solution concentration (C_e) at a constant-temperature is known as the adsorption isotherm [32]. Developing an appropriate isotherm model for adsorption is essential in designing and optimizing of adsorption processes [33]. For evaluating the equilibrium adsorption of compounds from solutions, several isotherm models have been developed such as Langmuir [34], Freundlich [35], Redlich-Peterson [36], Dubinin-Radushkevich [37] and Temkin [38] models. The more common models used to investigate the adsorption isotherm are Langmuir and Freundlich. The amount of a dye adsorbed onto [C_8MIM]-Fe_3O_4 nanoparticles was calculated based on the following mass balanced equation:

$$q_e = \frac{V(C_0 - C_e)}{m}$$

where q_e (in mg g^{-1}) is the adsorption capacity (mg dye adsorbed per gram [C_8MIM]-Fe_3O_4), V is the volume

of the dye solution (in liter), C_0 and C_e are the initial and equilibrium dye concentrations (in mg L^{-1}), respectively, and m is the mass (in gram) of dry [C_8MIM]-Fe_3O_4 nanoparticles added.

The equilibrium adsorption data of RR141 and RY81 were analyzed using Langmuir and Freundlich models. Model-fitting to equilibrium adsorption results of both dyes were assessed based on the values of the correlation coefficient (R^2) of the linear regression plot. The experimental data were fit with both models; the resulting plots are shown in Fig. 10.

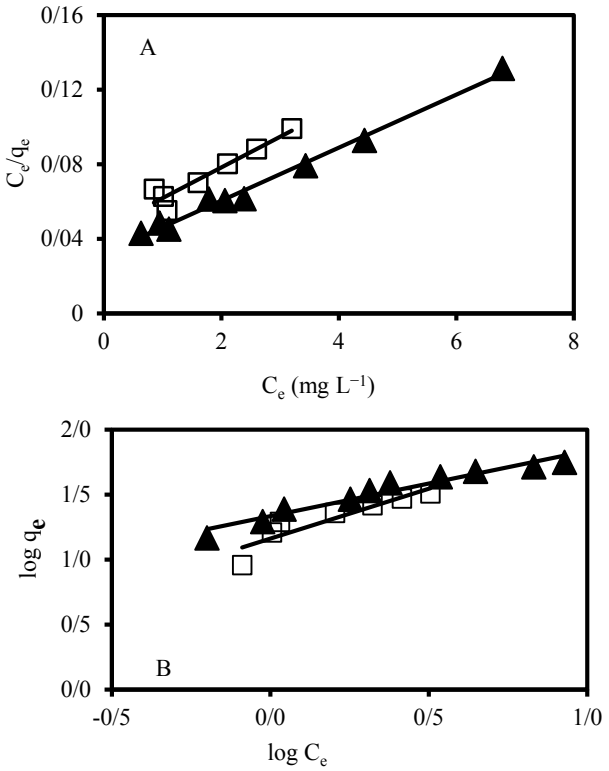

Fig. 10. (A), Langmuir isotherm plots; (B), Freundlich isotherm plots for adsorption of RR 141 (▲) and RY 81(□) onto [C_8MIM]-Fe_3O_4 nanoparticles. Experimental conditions: [C_8MIM]-Fe_3O_4 amount of 10 mg, initial pH 2.5, stirring time of 5 minute, initial dye concentration of 50-120 mg L^{-1}).

Table 3 summarizes the models constants and the correlation coefficients. As shown in Table 3, the R^2 of the Langmuir isotherm was greater than that of the Freundlich isotherm for the adsorption of both investigated dyes. This indicates that the adsorptions of RR141 and RY81 on [C_8MIM]-Fe_3O_4 nanoparticles are better described by the Langmuir model. This in turn suggests that adsorption occurs as the monolayer dyes adsorb onto the homogenous adsorbent surface. Table 3 shows that the maximum adsorption capacity for RR141 and RY81 are 71.4 and 62.5 mg dye per gram [C_8MIM]-Fe_3O_4, respectively. It should be mentioned that the dye adsorption process is affected by the properties of both dyes and adsorbent as reported [39]. The difference in adsorption removal of RR141 and RY81 may be attributed to their chemical structures and physical properties.

Table 4 presents a comparison between the proposed sorbent and other sorbents for the adsorption of both dyes [40-43].

3.7. Desorption

For potential applications, the regeneration of an adsorbent is important factor to be reported. Possible desorption of RR141 and RY81 was tested by using different solutions such as mixed methanol/acetic acid solution (with different volume ratios of 1:1, 2:1 and 1:2), pure methanol, sodium chloride solution (0.05, 0.1 and 1.0 mol L^{-1}), sodium hydroxide solution (0.05, 0.1 and 1.0 mol L^{-1}) and mixed sodium chloride (1.0 mol L^{-1})/acetone (with volume ratios of 1:1, 2:1 and 1:2). The study revealed that the adsorbed RR141 and RY81 could be completely desorbed in the presence of sodium chloride solutions with concentrations of 0.05 and 0.1 mol L^{-1}, respectively at 80 and 30 °C. Addition of desorbing solution in multiple steps (3 steps as was obtained) can improve the desorption process as expected.

4. CONCLUSION

A novel magnetic nano-adsorbent was fabricated by modifying the surface of Fe_3O_4 nanoparticles with [C_8MIM][Br]. The TEM and XRD analysis indicated that the surface modification resulted in the agglomeration of Fe_3O_4 nanoparticles with average diameter of ~13 nm, which did not change the structure of Fe_3O_4. The FTIR analysis demonstrated that the attachment of [C_8MIM][Br], on the surface of Fe_3O_4 nanoparticles, was achieved via the interaction between the cationic part of [C_8MIM][Br] and the surface hydroxyl groups of Fe_3O_4. The results obtained by immersion technique confirmed the binding of ionic liquid on the surface of Fe_3O_4 nanoparticles. It also revealed a pH shift for the point of zero charge (pH_{pzc}) from 6.5 to 8.0 after surface modification. The results of this study indicate that magnetic nanoparticles of [C_8MIM]-Fe_3O_4 have potential application in removal of RR141 and RY81 from wastewaters. Short contact time, high adsorption capacity, stability and reusability are advantages of [C_8MIM]-Fe_3O_4 nanoparticles as adsorbent. The adsorption of the tested dyes on the surface of [C_8MIM]-Fe_3O_4 nanoparticles was concluded to be attributed to the surface electrostatic and/or hydrophobic interactions between dyes and [C_8MIM]-Fe_3O_4 nanoparticles. The time required to achieve the adsorption equilibrium was 2 and 4 minutes for RY81 and RR141, respectively. The experimental data indicated that the adsorptions of both dyes on [C_8MIM]-Fe_3O_4 nanoparticles are better described by the Langmuir model. The maximum adsorption capacity of [C_8MIM]-Fe_3O_4 and Langmuir adsorption constant, respectively, were 71.4 mg $g^{-1}$and 0.31 L mg^{-1} for RR141. These parameters were 62.5 mg g^{-1} and 0.5 L mg^{-1}, respectively, for RY81. The absolute changes of enthalpy (ΔH) were determined to be 30.4 and −64.3 kJ mo^{-1} for RR141 and RY81, in the same order.

Table 3. Adsorption isotherms parameters of RR 141 and RY 81 onto [C_8MIM]-Fe_3O_4 nanoparticles.

	Langmuir model			Freundlich model		
Dye	q_{max}	b	R^2	K_F	n	R^2
RR141	71.4	0.31	0.988	21.6	1.99	0.944
RY81	62.5	0.50	0.916	14.5	1.30	0.873

Table 4. Comparisons of the proposed sorbent and other sorbents for the adsorption of both dyes.

Sorbent	Dye	Adsorption capacity (mg g^{-1})	Contact time	Reference
Metal hydroxide sludge	RR 141	51.5 (30 ºC)	1 h	[40]
WBA/H_2O	RR 141	24.3 (30 ºC)	24 h	[41]
WBA/H_2SO_4	RR 141	29.9 (30 ºC)	24 h	[41]
Activated carbon	RR 141	41.5 (30 ºC)	24 h	[41]
Chitin	RR 141	133 (30 ºC)	6 h	[42]
Modified chitin	RR 141	124 (30 ºC)	6 h	[42]
Spirogyra majuscula	RY 81	301.2	48 h	[43]
[C_8MIM]-Fe_3O_4	RR 141	71.4	4 min	This work
	RR 81	62.5	2 min	

ACKNOWLEDGMENTS

The authors wish to acknowledge the support of this work by Payame Noor University. We would like to thank Prof. G. Absalan, Department of Physics, Department of Engineering and Veterinary College at Shiraz University for their technical assistance.

REFERENCES

[1] T. Robinson, G. Mc Mullan , R. Marchant and P. Nigam, Remediation of dyes in textile effluent: a critical review on current treatment technologies with a proposed alternative, *Bioresour. Technol*. 77 (2001) 247-255.

[2] P. Cooper, Removing colour from dye house waste waters a critical review of Technology available, *J. Soc. Dyers Colour.* 109 (1993) 97-100.

[3] Y.M. Slokar, A. Majce and Le Marechal, Methods of decoloration of textile wastewaters, *Dyes Pigm*. 37 (1998) 335-356.

[4] P.K. Malik, Dye removal from wastewater using activated carbon developedfrom sawdust: adsorption equilibrium and kinetics, *J. Hazard. Mater.* B113 (2004) 81-88.

[5] E. Demirbas, M. Kobya and M.T. Sulak, Adsorption kinetics of a basic dye from aqueous solutions onto apricot stone activated carbon, *Bioresour. Technol*. 99 (2008) 5368-5373.

[6] D.D. Asouhidou, K.S. Triantafyllidis, N.K. Lazaridis, K.A. Matis, S.S. Kim and T.J. Pinnavaia, Sorption of reactive dyes from aqueous solutions by ordered hexagonal and disordered mesoporous carbons, *Micropor. Mesopor. Mater.* 117 (2009) 257-267.

[7] S.D. Lambert, N.G.D. Graham, C.J. Sollars and G.D. Fowler, Evaluation of inorganic adsorbents for the removal of problematic textile dyes and pesticides, *Water Sci. Technol*. 36 (1997) 173-180.

[8] N.K. Lazaridis, Karapantsios and T.D. Georgantas, Kinetic analysis for the removal of a reactive dye from aqueous solution onto hydrotalcite by adsorption, *Water Res*. 37 (2003) 3023-3033.

[9] M.S. Chiou and H.Y. Li, Equilibrium and kinetic modeling of adsorption of reactive dye on cross-linked chitosan beads, *J. Hazard. Mater*. 93 (2002) 233-248.

[10] X.S. Wang, Y. Zhou, Y. Yiang and C. Sun, The removal of basic dyes from aqueous solutions using agricultural by-products*, J. Hazard. Mater.* 157 (2008) 374-385.

[11] F. Cicek, D. Ozer and A. Ozer, Low cost removal of reactive dyes using wheat bran, *J. Hazard. Mater*. 146 (2007) 408-416.

[12] S. Pirillo, M.L. Ferreira and E.H. Rueda, Adsorption of alizarin, eriochrome blue black R, and fluorescein using different iron oxides as adsorbents, *Ind. Eng. Chem. Res*. 46 (2007) 8255-8263.

[13] A. Afkhami and R. Moosavi, Adsorptive removal of Congo red, a carcinogenic textile dye, from aqueous solutions by maghemite nanoparticles, *J. Hazard. Mater.* 174 (2010) 398-403.

[14] P. Bonhote, A.P. Dias, N. Papageorgion, K. Kalyanasundaran and M. Gratzel, Highly conductive ambient-temperature molten salts, *Inorg. Chem*. 35 (1996) 1168-1178.

[15] D.K. Kim, Y. Zhang, W. Voit, K.V. Rao and M. Muhammed, Synthesis and characterization of surfactant-coated superparamagnetic monodispersed iron oxide nanoparticles, J. *Magn. Magn. Mater*. 225 (2001) 30-36.

[16] S.I. Park, J.H. Kim, , J.H. Lim, C.O. Kim, Surface-modified magnetic nanoparticles with lecithin for applications in biomedicine, *Curr. Appl. Phys.* 8 (2008) 706-709.

[17] D. Faivre and P. Zuddas,. An integrated approach for determining the origin of magnetite nanoparticles, Earth Planet. *Sci. Lett*. 243 (2006) 53-60.
[18] R.D. Waldron, Infrared spectra of ferrites, *Phys. Rev*. 99 (1955) 1727-1735.
[19] K. Can, M. Ozmen and M. Ersoz, Immobilization of albumin on aminosilane modified superparamagnetic magnetite nanoparticles and its characterization, *Colloids Surf. B Biointerfaces* 71 (2009) 154-159.
[20] N. Foil and I. Villaescusa, Detremination of sorbent point zero charge: usefulness in sorption studies, *Environ. Chem. Lett*. 7 (2009) 79-84.
[21] M.T. Uddin, M.A. Islam, S. Mahmud and M. Rukanuzzaman, Adsorptive of removal of methylene blue by tea waste, *J. Hazard. Mater*. 164 (2009) 53-60.
[22] M. Constantin, I. Asmarandei , V. Harabagiu, L. Ghimici, P. Ascenzi and G. Fundueanu, Removal of anionic dyes from aqueous solutions by an ion-exchanger based on pullulan microspheres, *Carbohyd. Polymers* 91 (2013) 74-84.
[23] B.H. Hameed, A.A. Ahmad and N. Aziz. Isotherms, kinetics and thermodynamics of acid dye adsorption on activated palm ash, *Chem. Eng. J.* 133 (2007) 195-203.
[24] A. Özcan and A. Safa Özcan, Adsorption of Acid Red 57 from aqueous solutions onto surfactant-modified sepiolite, *J. Hazard. Mater. B* 125 (2005) 252–259.
[25] J. Li , X. Zhao, Y. Shi, Y. Cai, S. Mou and G. Jiang, Mixed hemimicelles solid-phase extraction based on cetyltrimethylammonium bromide-coated nano-magnets Fe_3O_4 for the determination of chlorophenols in environmental water samples coupled with liquid chromatography/spectrophotometry detection, *J. Chromat. A,* 1180 (2008) 24-31.
[26] N.M. Mahmoodi and B.M. Hayati, Bovine serum albumin (BSA) adsorption with Cibacron Blue F3GA attached chitosan microspheres, *Ind. Crop. Prod*. 35 (2012) 295-301.
[27] B. Saha, S. Das, J. Saikia and G. Das, Preferential and enhanced adsorption of different dyes on iron oxide nanoparticles, *J. Phys. Chem*. *C* 11 (2011) 8024-8033.
[28] S. Kamran, M. Asadi and G. Absalan, Adsorption of acidic, basic, and neutral proteins from aqueous samples using Fe_3O_4 magnetic nanoparticles modified with an ionic liquid, *Microchim. Acta* 108 (2013) 41-48.
[29] Z. Zhang, I.m. O'Hara, G.A. Kent and W.O.S. Doherty, Comparative study on adsorption of two cationic dyes by milled sugarcane Bagasse, *Ind. Crop. Prod*. 42 (2013) 41-49.
[30] M. Ghaemi and G. Absalan, Study on the adsorption of DNA on Fe_3O_4 nanoparticles and on ionic liquid-modified Fe_3O_4 nanoparticles, *Microchim. Acta* 181 (2014) 45-53.
[31] G. Absalan, S. Kamran, M. Asadi, L. Sheikhian and D. M. Goltz, Removal of reactive red-120 and 4-(2-pyridylazo) resorcinol from aqueous samples by Fe_3O_4 magnetic nanoparticles using ionic liquid as modifier, *J. Hazard. Mater*. 192 (2011) 476-484.
[32] S. Chatterjee, D.S. Lee and S.H. Wooa, Enhanced adsorption of congo red from aqueous solution by chitosan hydrogel beads impregnated with cetyltrimethyl ammonium bromide, *Bioresour. Technol*. 100 (2009) 2803-2809.
[33] I.A.W. Tan, A.L. Ahmad and B.H. Hameed, Adsorption of basic dye on high-surface area activated carbon prepared from coconut husk: equilibrium, kinetic and thermodynamic studies*, J. Hazard. Mater*. 154 (2008) 337-346.
[34] I. Langmuir, The adsorption of gases on plane surfaces of glass, mica and platinum, *J. Am. Chem. Soc*. 40 (1918) 1361-1403.
[35] H.M.F. Freundlich, Over the adsorption in solution, *J. Phys. Chem.-US 57* (1906) 385-471.
[36] O. Redlich and D.L. Peterson, A useful adsorption isotherm, *J. Phys. Chem*. 63 (1959) 1024-1026.
[37] T.P.O. Connor and J. Muller, Modeling competitive adsorption of chlorinated volatile organic compounds with the Dubinin-Radushkevich equation, *Micropor. Mesopor. Mater*. , 46 (2001) 341-349.
[38] J.H. Chun, S.K. Jeon, N.Y. Kim and J.Y. Chun, The phase-shift method for determining Langmuir and Temkin adsorption isotherms of over-potentially deposited hydrogen for the cathodic H_2 evolution reaction at the poly-Pt/H_2SO_4 aqueous electrolyte interface, *Int. J. Hydrogen Energy* 30 (2005) 1423-1436.
[39] V. Rocher, J.M. Siaugue, V. Cabuil and A. Bee, Removal of organic dyes by magnetic alginate beads, *Water Res*. 42 (2008) 1290-1298.
[40] S. Netpradit, P. Thiravetyan and S. Towprayoon, Adsorption of three azo reactive dyes by metal hydroxide sludge:effect of temperature, pH and electrolytes, *J. Colloid Interf. Sci*. 270 (2004) 255-261.
[41] P. Leechart, W. Nakbanpote and P. Thiravetyan, Application of 'waste' wood-shaving bottom ash for adsorption of azo reactive dye, *J. Environ. Manag.* 90 (2009) 912-920.
[42] R. Dolphen, N. Sakkayawong, P. Thiravetyan and W. Nakbanpote, Adsorption of Reactive Red 141 from wastewater onto modified chitin*, J. Hazard. Mater*. 145 (2007) 250-255.
[43] A. Çelekli, M. Yavuzatmaca and H. Bozkurt, Binary adsorption of reactive red 120 and yellow 81 on spirogyra majuscula, *Middle East J. Sci. Res.* 13 (2013) 740-748.